Scripta Materialia 207 (2022) 114260

Contents lists available at ScienceDirect

Scripta Materialia

journal homepage: www.elsevier.com/locate/scriptamat

A new $\alpha + \beta$ Ti-alloy with refined microstructures and enhanced mechanical properties in the as-cast state

Tianlong Zhang[a,b], Jiaming Zhu[a], Tao Yang[a], Junhua Luan[a], Haojie Kong[a], Weihong Liu[a,c], Boxuan Cao[a], Shiwei Wu[a], Dong Wang[b], Yunzhi Wang[d], Chain-Tsuan Liu[a,*]

[a] Department of Materials Science and Engineering, College of Engineering, Hong Kong Institute for Advanced Study, City University of Hong Kong, Tat Chee Avenue, Kowloon Tong, Kowloon, China
[b] Frontier Institute of Science and Technology, State Key Laboratory for Mechanical Behavior of Materials, Xi'an Jiaotong University, Xi'an 710049, China
[c] School of Materials Science and Engineering, Harbin Institute of Technology (Shenzhen), Shenzhen, China
[d] Department of Materials Science and Engineering, The Ohio State University, 2041 College Road, Columbus, OH 43210, USA

ARTICLE INFO

Article history:
Received 22 June 2021
Revised 23 August 2021
Accepted 30 August 2021

Keywords:
Titanium alloys
Mechanical property
Grain refinement
Thermodynamic calculation
Alloy design

ABSTRACT

A new (α + β) Ti-alloy, Ti-6Al-2V-1Cr-1Fe (wt%), with fine grain sizes, fine precipitates, together with the high strength and excellent ductility in its as-cast state is developed. As compared to the as-cast commercial Ti-6Al-4V alloy, the grain size and α lath thickness of the new alloy are substantially refined by 50∼75%, and the yield strength and ductility are increased by 19.7% and 51.8%, respectively. The grain size refinement is achieved by tuning the supercooling capacity of the alloy through alloying with the aid of CALPHAD calculations. In addition, the alloying of Cr and Fe substantially reduces the α lath thickness. This low-cost Ti alloy with the enhanced properties is anticipated to be highly suitable for various structural applications in its as-cast or as-printed state.

Titanium alloys are among the most important structural materials due to their high specific strength and excellent corrosion resistance [1,2]. However, their applications are mostly limited to high-end advanced systems, such as aircraft and submarines [3,4], due to the high raw material cost and high buy-to-fly ratio [1]. Furthermore, the relatively poor machinability of most Ti alloys substantially increases their production cost during manufacturing [5]. Thus, the development of low-cost and high-performance Ti alloys with a net-shape manufacturing capability is imperative [6,7]. Casting is a mature and effective near-net-shape processing technology, and pure Ti and Ti-6Al-4V components of complicated geometries have been cast routinely for cost-sensitive applications with low wastes [8]. Nevertheless, a major problem associated with the cast Ti and its alloys is their coarse grain and precipitate microstructures, as well as the relatively poor mechanical properties [1,8]. For example, the widely used cast Ti64 alloy, which even has a matched strength, shows a substantially inferior tensile ductility [9] to its wrought counterpart. This is because most Ti alloys (including the Ti64 alloy) are originally designed for the wrought process, without optimization of their microstructures at the as-cast state [9–11].

The Ti64 alloy in its as-cast state has been characterized as large grains and coarse α colonies, which are responsible for its relatively poor mechanical properties [1,2]. For casting applications, for the consideration of no thermomechanical treatments allowable after the casting process and the requirement of minimized post-heat treatment procedures for a cost reduction, it becomes critically important to optimize the alloy composition for microstructural control in its as-cast state. Alloying is an effective way to alter the microstructure morphology for mechanical property enhancement. The main objective of this study is thus to develop a new-type strong and ductile cast Ti alloy with the aid of CALPHAD (calculation of PHAse Diagrams) method. The choice of the alloying elements in this study are based on the following considerations: (1) their ability in the grain size refinement during casting; (2) their effect on the α precipitate microstructure shift as well as volume fraction change of the α and β phases; (3) absence of brittle intermetallic phases, and (4) low cost of raw alloying elemental materials. Considering the high cost and bad oxidation/sulfidation resistance of the *V* element, its content should be reduced in the baseline alloy Ti64 and replaced by Cr and Fe. The Fe and Cr elements are also selected for their ability in the microstructure shift.

For alloy composition optimization in this study, we first combined the thermodynamic calculations with nucleation theories

* Corresponding author.
E-mail address: chainliu@cityu.edu.hk (C.-T. Liu).

https://doi.org/10.1016/j.scriptamat.2021.114260
1359-6462/

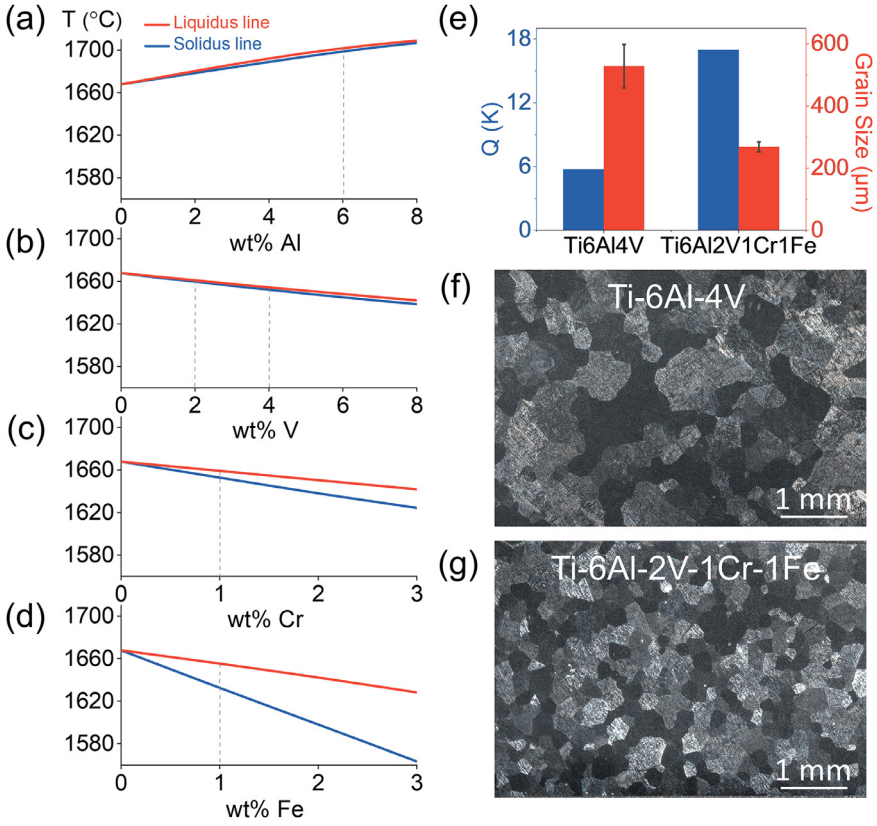

Fig. 1. (a–d) Ti-X (Al, V, Fe, Cr) binary phase diagrams calculated by Thermo-Calc. (e) Calculated growth restriction factor Q of Ti-6Al-4V and Ti-6Al-2V-1Cr-1Fe alloys (blue bars) and experimental statistical results of the average grain size in (f) and (g). Optical micrograph of the grain structure of (f) Ti-6Al-4V and (g) Ti-6Al-2V-1Cr-1Fe alloys (For interpretation of the references to color in this figure legend, the reader is referred to the web version of this article).

to evaluate the effect of alloying elements on the grain size refinement and phase constitution. The Thermo-Calc 3.1 software [10] with the TTTI3 Ti-based thermodynamic database was used for such calculations. The as-cast Ti-alloys were fabricated by arc melting under a Ti-gettered high-purity argon atmosphere and were repeatedly melted for 5 times before casting into a 70*12*5 mm^3 copper mold. The high purity elemental materials with a purity of at least 99.9% were used. The ingots were then machined into the standard dog-bone tensile specimens by a wire-electrode cutting machine with a gauge length of 12.5 mm. The tensile samples were mechanically polished to a final 5000 grit surface finish before tensile tests at room temperature. The Material testing system (MTS) tensile testing machine equipped with an MTS 10 mm extensometer was used for room temperature tensile test at a strain rate of 10^{-3} s^{-1}. Three tensile samples were tested to confirm reproducibility, and the average values were reported. The yield strength was determined with the 0.2% offset plastic strain method. For microstructure characterizations, the samples were first polished to a final 5000 grit surface finish by SiC papers and then polished electronically to a bright mirror finish. The polishing solution used for our titanium alloys is HNO_3: Methanol (1:3). And the polisher was set to 22 V and the temperature was kept at -20 °C. Microstructure analysis was performed using an FEI Quanta 450 scanning electron microscope (SEM). The Rigaku SmartLab X-ray diffraction (XRD) instrumented by Cu-K_α radiation with a scan speed of 2 °/min is used for phase identification.

Most as-cast Ti-alloys tend to form coarse/columnar grains during rapid cooling from their liquid state. To refine the grain structure without deformation + recrystallization via additional thermomechanical processing, the common method used is to introduce external grain refiners, such as La_2O_3, TiC, etc [6,12]. To promote heterogeneous nucleation during solidifications. However, these particles are easily agglomerate and usually harmful to their mechanical properties (especially the tensile ductility). The other method, which has mostly been overlooked and underutilized, is to control the supercooling capacity of the Ti alloys by alloy design. To evaluate the effects of various elements, several Ti-X (Al, V, Fe, Cr) binary phase diagrams are calculated (as shown in Fig. 1(a–d)). And the growth restriction factor Q is calculated as [13]:

$$Q = c_0 m(k-1) \quad (1)$$

where c_0 represents the solute concentration, m is the slope of the liquidus line in the phase diagram and k is the solute partition coefficient. The partitioning coefficient k is calculated by the equation of $k = C_S/C_L$ based on the calculated phase diagram (where C_S and C_L are the compositions of solid and liquid, respectively.). It is clear that, when compared with Al and *V*, the addition of Fe and Cr elements in Ti alloys substantially raises the solidification range ΔT in the liquid + β phase region. Since the k value is closely related to the solidification range, a larger solidification range always leads to a larger deviation of the values of k from its ideal value of 1 and consequently results in a larger Q value. As shown in Fig. 1(e), by replacing 2 wt% of *V* in Ti64 with 1 wt% of Fe and 1 wt% Cr, the Q value of the alloy increases from 5.7 to 16.9 K. Thus, Fe and Cr are predicted to be better grain refiners for the Ti64 alloy. Experimental results (statistic results in Fig. 1(e) and microstructure images in Fig. 1(f, g)) verify that comparing to typical as-cast Ti64 alloy having a large grain size of 528 ± 70 μm, our newly designed Ti-6Al-2V-1Cr-1Fe alloy shows a relatively refined grain structure of 268 ± 16 μm in its as-cast state. It can be reasonably inferred that more Cr and Fe additions can further refine the grain structure to < 100 μm. However, the excessive Cr and Fe would lead to the formation of the extremely brittle $TiCr_2$ or TiFe intermetallic

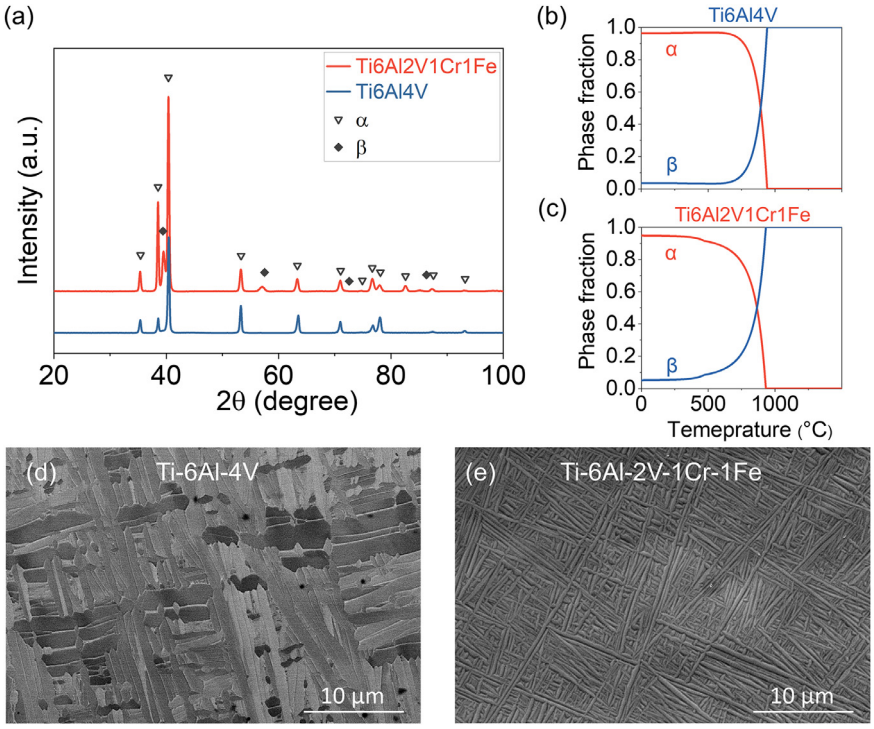

Fig. 2. (a) X-ray diffraction patterns of the as-cast Ti-6Al-2V-1Cr-1Fe (red) and Ti-6Al-4V (blue) alloys. The abbreviation "a.u." represents arbitrary units. Calculated phase fraction as a function of the temperature of the (b) Ti-6Al-4V and (c) Ti-6Al-2V-1Cr-1Fe alloys. Scanning electron microscope (SEM) images showing a fully lamellar microstructure of the as-cast (d) Ti-6Al-4V and (e) Ti-6Al-2V-1Cr-1Fe alloys (For interpretation of the references to color in this figure legend, the reader is referred to the web version of this article).

phases [1,7] and will seriously damage the ductility of the material [14]. In addition, excessive alloying elements may increase the segregation tendency during solidification, which may reduce the castability. Thus, the Cr and Fe contents are both confined to 1 wt% in the newly designed Ti-6Al-2V-1Cr-1Fe alloy.

The alloying elements also tune the phase constituent of the Ti alloy. Since the Cr and Fe elements are stronger β-stabilizers than the *V* element in Ti alloys [2]. Besides the grain refinement, the addition of Cr and Fe elements leads to a higher volume fraction of the β phase than that in the Ti64 alloy. As shown by the XRD patterns in Fig. 2(a) (for comparing to the base Ti64 alloy), the as-cast Ti-6Al-2V-1Cr-1Fe alloy shows the higher peak intensity of $(110)_\beta$ at 39.4 ° and $(200)_\beta$ at 57.5 °. According to the XRD results [15], the β phase fraction is estimated to be ~20.3% in the as-cast Ti-6Al-2V-1Cr-1Fe and < 5% in the Ti64 alloy. Need to note that the β phase fraction estimated by the XRD patterns shows a small deviation from the Thermo-calc calculations at the room temperature (Fig. 2(b, c)). On the one hand, the precision of the estimation calculation relies on the accuracy of our experimental measurements and also the PDF card in the XRD databases. On the other hand, and more importantly, the non-equilibrium nature of the casting process will always preserve a larger fraction of the high-temperature phase during the fast cooling. Thus, the actual volume fraction of the β phase in the as-cast state is closer to the theoretical value at ≥ 500 °C. Since the β phase (body-centered-cubic structure, bcc) has more slip systems than that in the α phase (hexagonal closest packed structure, hcp), the increased β phase fraction is anticipated to bear a more plastic deformation when strained and is beneficial to the overall ductility [16].

Another interesting effect of the Cr and Fe additions is the α precipitates' morphology shift. As shown in Fig. 2(d, e), the average α lath thickness drastically decreases from ~1.2 ± 0.2 μm in the Ti64 alloy to ~0.3 ± 0.1 μm in the Ti-6Al-2V-1Cr-1Fe alloy. As compared to the Ti64 alloy, the aspect ratio of the α precipitates in the Ti-6Al-2V-1Cr-1Fe alloy is also much higher. More importantly, conventional as-cast Ti64 alloys usually show a large α colony structure [1]. Within the individual α colonies, the α lamellas own the same orientation (microtexture), which is remarkably harmful to the strength and fatigue properties of Ti alloys [2]. While in the as-cast Ti-6Al-2V-1Cr-1Fe alloy, the coarse α colonies are completely eliminated. Instead, a basketweave microstructure appears.

The much refined microstructure of the Ti-6Al-2V-1Cr-1Fe alloy exhibits excellent mechanical properties as shown in Fig. 3(a). The as-cast Ti-6Al-2V-1Cr-1Fe alloy exhibits a high yield strength of 1057 ± 39 MPa and an excellent tensile elongation of 8.5 ± 0.6%. Comparing to the commonly used Ti64 alloy (blue curve in Fig. 3(a)), the newly designed Ti-6Al-2V-1Cr-1Fe alloy shows the simultaneously increased strength and ductility (the yield strength and ductility are increased by 19.7% and 51.8%, respectively). Need to note that the high Cr/Fe alloys (gray and yellow curves in Fig. 3(a)) exhibit a higher strength but very limited ductility due to the formation of brittle intermetallic compounds [6,7].

As mentioned above, the increased ductility is a result of the increased β phase fraction [6,17], as well as a refined grain structure [18]. While the increased strength is attributed to a synergistic effect of three mechanisms: solid solution strengthening, Hall-Petch effect, and fine precipitation strengthening (Fig. 3(b)). Firstly, the solid solution strengthening is usually considered as one of the main strengthening mechanisms in Ti alloys [19,20], and among all kinds of solute elements, Fe and Cr are much stronger solid solute strengthening elements than *V* [19,21]. The strengthening effect of solute elements in solid solutions is originally carried out by Fleisher [22] and developed by Labusch as [23]:

$$\sigma_{ss} = B_i X_i^{2/3} \quad (2)$$

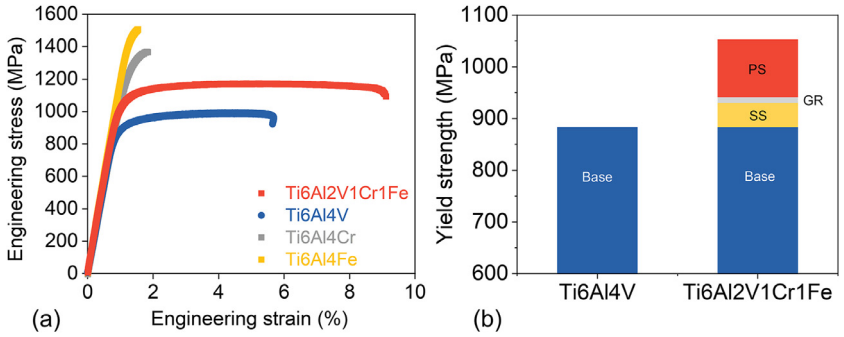

Fig. 3. (a) Engineering stress-strain curves of the as-cast Ti-6Al-2V-1Cr-1Fe (red), Ti-6Al-4V (blue), Ti-6Al-4Cr (gray) and Ti-6Al-4Fe (yellow) alloys. (b) Schematic diagram showing the origin of the yield strength increment during composition optimization in Ti-6Al-2V-1Cr-1Fe, as compared with Ti-6Al-4V. PS: fine precipitation strengthening; GR: Hall-Petch effect by grain refinement; SS: solid solution strengthening (For interpretation of the references to color in this figure legend, the reader is referred to the web version of this article).

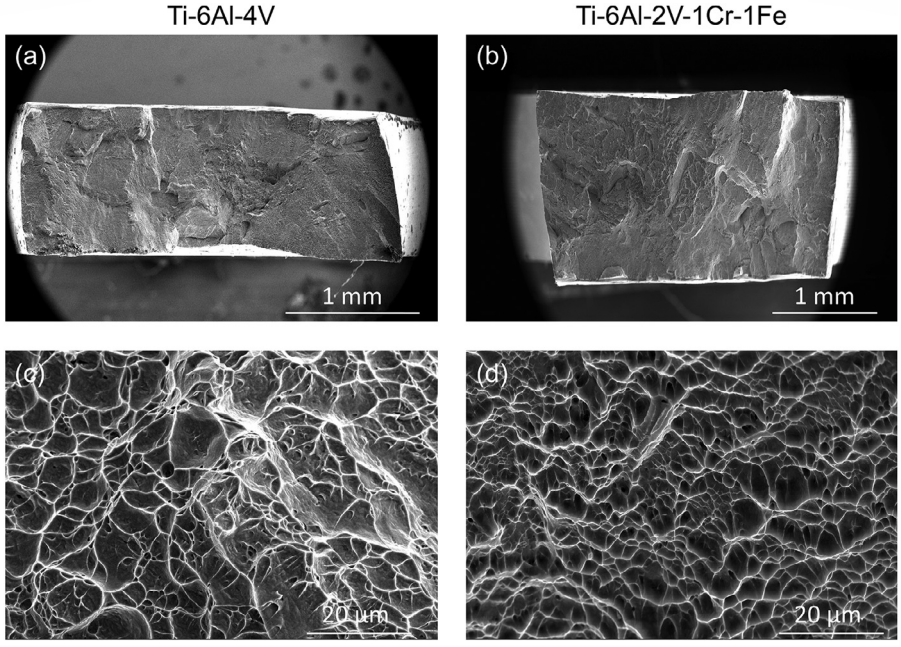

Fig. 4. Fracture surfaces of the as-cast (a) Ti-6Al-4V and (b) Ti-6Al-2V-1Cr-1Fe alloys. Higher magnification of the fracture surfaces showing various dimple patterns of the as-cast (c) Ti-6Al-4V and (d) Ti-6Al-2V-1Cr-1Fe alloys.

where B_i is the strengthening coefficient for the solute i and X_i is the atomic concentration of the solute i. For our dual phase Ti-alloy, the strength formulation then takes the form [19]:

$$\sigma_{ss} = f_\alpha \times \left(\sum_i B_i^{3/2} X_{i,\ \alpha} \right)^{2/3} + f_\beta \times \left(\sum_i B_i^{3/2} X_{i,} \right)^{2/3} \quad (3)$$

where f_α and f_β are the fractions of the α and β phases, respectively. Thus, setting the strength of the base Ti64 alloy as the base strength and taking the strengthening coefficient from Ref. [19], we derive the strength increment due to the substitution of 2 wt% of V by 1 wt% of Cr and 1 wt% of Fe in the new alloy as $\Delta\sigma_{ss} = \sigma_{ss,\ Ti6211} - \sigma_{ss,\ Ti64}$=46.9 MPa [19]. Consequently, the solid solution strengthening contributes to a great part in the strength increment during the compositional optimization of the new alloy as compared to the Ti64 alloy.

Secondly, the increased strength due to the grain refinement is given by the classic Hall-Petch relationship as:

$$\Delta\sigma_g = k_y \left(\frac{1}{\sqrt{d_{Ti6211}}} - \frac{1}{\sqrt{d_{Ti64}}} \right) \quad (4)$$

where k_y is the strengthening coefficient and d is the average grain diameter. The Hall–Petch coefficient in Ti-alloys ranges from 0.5 to 0.7 MN $m^{-3/2}$ [1]. Thus, comparing to the base Ti64 alloy, the extra fine grain strengthening due to the higher supercooling capacity is estimated to be ~11 MPa.

Thirdly, it has been generally concluded that the α/β interface can effectively resist the dislocation slip during deformation. Thus, the α precipitates' morphology is also considered to be one of the most effective factors that influence the strength of Ti alloys [1,24,25]. Welk [26] and Collins et al. [27] have systematically studied the complex effect of the α lath thickness on the strength of Ti alloys. Combining both the computational studies and the statistical experimental results [2,26–29], we derive an empirical relationship between the α lath thickness and the yield strength as:

$$\sigma_\alpha = \sigma_0 - 122 * W_\alpha \quad (5)$$

where W_α represents the average thickness of the α lath and σ_0 is a constant. As expected, the refinement of the α lath thickness from 1.2 to 0.3 μm in the new alloy contributes the most to the strength increment with the value of ~ 108 MPa.

Based on the above analyzes, the strengthening effect of the alloying elements of Cr and Fe in terms of solid solution strengthening, grain size refinement, and precipitation strengthening are summarized in Fig. 3(b). The sum of the calculated strength increment shows a small deviation from the experimental values, which validates the reliability of these models. The major increase of the yield strength in the newly designed Ti-6Al-2V-1Cr-1Fe alloy is due to the refined α lath, solid solute strengthening, and followed by the finer grain size.

Further investigation on the fracture surfaces (see Fig. 4) corresponds well with the stress-strain curve in Fig. 3(a). Both the Ti64 and Ti-6Al-2V-1Cr-1Fe alloys show a clear dimple pattern, indicating a ductile fracture mode. No obvious cleavage or intergranular fracture is detected. Comparing with the Ti64 alloy, the average dimple size in the as-cast Ti-6Al-2V-1Cr-1Fe alloy appears to be more uniform and smaller, and the proportion of the bimodal dimples appear to be more reduced [30].

It should be pointed out that our study is the first step of studying such new kinds of Ti alloys. Though the Ti-6Al-2V-1Cr-1Fe alloy is designed for the casting process, further thermomechanical treatments or post-heat treatment can also be applied to modify the microstructures. By tailoring the grain size and α precipitate morphology, or eliminating the casting defects, further improvements of the strength, ductility, fatigue, toughness, etc. balance for more application scenarios, can be expected.

In summary, our work has demonstrated a new strategy to design a strong and ductile as-cast Ti alloy with the aid of the CALPHAD calculations. By substituting 1 wt% of Cr and Fe, the increased supercooling capacity of the Ti-6Al-2V-1Cr-1Fe results in the substantially refined grain size during solidification without a macrosegregation of the casting ingot. The refined grain structure, α lath thickness, enhanced solid solute strengthening, as well as a higher fraction of the retained β phase, synergistically contribute to the simultaneous increase of the strength and ductility of the Ti alloy. Furthermore, the new cost-effective alloy containing only 2% instead of 4% Vanadium, is expected to enhance the corrosion resistance to the alloy. Our approach not only develops a kind of promising as-cast Ti alloy that can replace the widely-used casting Ti64 alloy in the industry, but also proposes a powerful strategy in designing new generation metallic materials for microstructure optimization and property enhancement with near-net forming ability (e.g. casting, additive manufacturing, etc).

Declaration of Competing Interest

The authors declare that they have no known competing financial interests or personal relationships that could have appeared to influence the work reported in this paper.

Acknowledgments

The authors from City University of Hong Kong (CityU) are grateful for the internal funding from City University of Hong Kong under the Programs 9042635, 9360161, 9380060. The authors from Xi'an Jiaotong University would like to acknowledge the supported by the National Key Research and Development Program of China (Grants No. 2016YFB0701302) and the National Natural Science Foundation of China (Grants Nos. 51671156, 51671158). Y.W. would like to acknowledge the support by US national science foundation under Grant DMR - 1923929.

References

[1] D. Banerjee, J.C. Williams, Acta Mater. 61 (2013) 844–879.
[2] G. Lütjering, J.C. Williams, Titanium, Springer, New York, 2007.
[3] M. Peters, J. Kumpfert, C.H. Ward, C. Leyens, Adv. Eng. Mater. 5 (2003) 419–427.
[4] A.K. Sachdev, K. Kulkarni, Z.Z. Fang, R. Yang, V. Girshov, JOM 64 (2012) 553–565.
[5] E.O. Ezugwu, Z.M. Wang, J. Mater. Process. Technol. 68 (1997) 262–274.
[6] Z. Liang, J. Miao, T. Brown, A.K. Sachdev, J.C. Williams, A.A. Luo, Scr. Mater. 157 (2018) 124–128.
[7] J.H. Luan, Z.B. Jiao, W.H. Liu, Z.P. Lu, W.X. Zhao, C.T. Liu, Mater. Sci. Eng. A 704 (2017) 91–101.
[8] R.W. Cahn, The Coming of Materials Science, 1st ed., Elsevier Science, Kidlington, 2010.
[9] M. Niinomi, Mater. Sci. Eng. A 243 (1998) 231–236.
[10] L. Nastac, M.N. Gungor, I. Ucok, K.L. Klug, W.T. Tack, Int. J. Cast Met. Res. 19 (2006) 73–93.
[11] Qizhen Li, Edward Y. Chen, Douglas R. Bice, David C. Dunand, Metall. Mater. Trans. A 39 (2008) 441–449.
[12] M.J. Bermingham, D.H. StJohn, J. Krynen, S. Tedman-Jones, M.S. Dargusch, Acta Mater. 168 (2019) 261–274.
[13] D.H. StJohn, M. Qian, M.A. Easton, P. Cao, Acta Mater. 59 (2011) 4907–4921.
[14] C. Leyens, M. Peters, Titanium and Titanium Alloys: Fundamentals and Applications, Wiley, Weinheim, Chichester, 2003 [VCH; John Wiley] (distributor).
[15] C.R. Hubbard, R.L. Snyder, Powder Diffr. 3 (1988) 74–77.
[16] Z.C. Sun, H. Yang, G.J. Han, X.G. Fan, Mater. Sci. Eng. A 527 (2010) 3464–3471.
[17] J.H. Luan, Z.B. Jiao, G. Chen, C.T. Liu, J. Alloys Compd. 602 (2014) 235–240.
[18] Y. Chong, T. Bhattacharjee, J. Yi, A. Shibata, N. Tsuji, Scr. Mater. 138 (2017) 66–70.
[19] G.-H. Zhao, X.Z. Liang, B. Kim, P.E.J. Rivera-Díaz-del-Castillo, Mater. Sci. Eng. A 756 (2019) 156–160.
[20] P. Li, T. Zhang, X. Sun, H. Zhang, D. Wang, Q. Sun, L. Xiao, et al., Mater. Sci. Eng. A 759 (2019) 640–647.
[21] I. Ghamarian, B. Hayes, P. Samimi, B.A. Welk, H.L. Fraser, P.C. Collins, Mater. Sci. Eng. A 660 (2016) 172–180.
[22] R.L. Fleischer, Acta Mater. 11 (1963) 203–209.
[23] R. Labusch, Phys. Status Solidi B 41 (1970) 659–669.
[24] T. Zhang, D. Wang, Y. Wang, Acta Mater. 196 (2020) 409–417.
[25] A. Devaraj, V.V. Joshi, A. Srivastava, S. Manandhar, V. Moxson, V.A. Duz, C. Lavender, Nat. Commun. 7 (2016) 11176.
[26] Welk, Brian A. Microstructural and Property Relationships in β-Titanium Alloy Ti-5553: Masters thesis[D]. Ohio:The Ohio State University, 2010. Advisor: Hamish L. Fraser https://etd.ohiolink.edu/apexprod/rws_olink/r/1501/10?clear=10&p10_accession_num=osu1262191957.
[27] P.C. Collins, B. Welk, T. Searles, J. Tiley, J.C. Russ, H.L. Fraser, Mater. Sci. Eng. A 508 (2009) 174–182.
[28] J. Tiley, T. Searles, E. Lee, S. Kar, R. Banerjee, J.C. Russ, H.L. Fraser, Mater. Sci. Eng. A 372 (2004) 191–198.
[29] S. Kar, T. Searles, E. Lee, G.B. Viswanathan, H.L. Fraser, J. Tiley, R. Banerjee, Metall. Mater. Trans. A 37 (2006) 559–566.
[30] L. Ren, W. Xiao, H. Chang, Y. Zhao, C. Ma, L. Zhou, Mater. Sci. Eng. A 711 (2018) 553–561.